

# Liquefying Compounds by Forming Deep Eutectic Solvents: A Case Study for Organic Acids and Alcohols

Published as part of *The Journal of Physical Chemistry virtual special issue "Deep Eutectic Solvents"*.

Dinis O. Abranches, Renato O. Martins, Liliana P. Silva, Mônia A. R. Martins, Simão P. Pinho, and João A. P. Coutinho\*

Cite This: *J. Phys. Chem. B* 2020, 124, 4174–4184

Read Online

ACCESS |

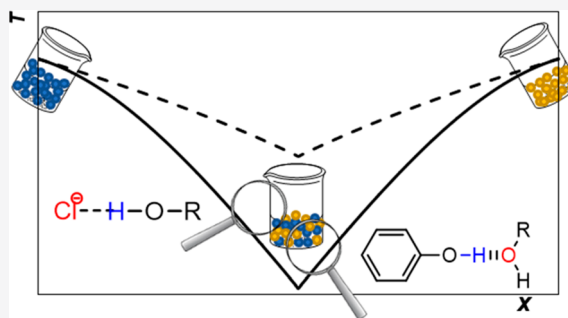
Metrics & More

Article Recommendations

Supporting Information

**ABSTRACT:** The criterion to distinguish a simple eutectic mixture from a deep eutectic solvent (DES) lies in the deviations to thermodynamic ideality presented by the components in the system. In this work, the current knowledge of the molecular interactions in types III and V DES is explored to liquefy a set of three fatty acids and three fatty alcohols, here used as model compounds for carboxyl and hydroxyl containing solid compounds. This work shows that thymol, a stronger than usual hydrogen bond donor, is able to form deep eutectic solvents of type V with the fatty alcohols studied. This is particularly interesting, since these DES formed are hydrophobic. Regarding type III DES, the results suggest that the prototypical DES hydrogen bond acceptor, cholinium chloride, is unable to induce negative deviations to ideality in the model molecules studied.

By substituting choline with tetramethylammonium chloride, it is shown that the choline hydroxyl group is responsible for the difficulty in forming choline-based deep eutectic solvents and that its absence induces strong negative deviations to ideality in the alkylammonium side. Finally, it is demonstrated that tetrabutylammonium chloride acts as a chloride donating agent, causing significant negative deviations to ideality in both fatty acids and alcohols and leading to the formation of deep eutectic solvents of type III.



## 1. INTRODUCTION

Deep eutectic solvents (DES) are a novel class of solvents<sup>1,2</sup> that emerged from the seminal works of Abbott and co-workers,<sup>2,3</sup> where it was reported that binary mixtures of cholinium chloride and urea or a series of carboxylic acids (malonic acid, phenylpropanoic acid, or phenylacetic acid) are liquid at room temperature. Putting it simply and despite some questionable exceptions also presented by Abbott et al.<sup>4,5</sup> using liquid components, eutectic solvents (ES) could be defined as liquid mixtures prepared from pure solid compounds. The liquid phase of ES arises due to the melting point depression of the system, which depends on the melting temperature and enthalpy of its components as well as their intermolecular interactions. The greater the negative deviations to thermodynamic ideality of both components, the greater the melting temperature depression, with the prefix *deep* here attributed to systems showing negative deviations to ideality.<sup>6</sup>

Deep eutectic solvents have found applications in a variety of scientific areas, such as extraction and separation,<sup>7–12</sup> reaction chemistry,<sup>13–16</sup> analytical chemistry,<sup>17</sup> biodiesel synthesis,<sup>18,19</sup> and electrochemistry.<sup>20</sup> Interestingly, cholinium chloride-based DES are by far the most studied in the literature,<sup>1–3,6–21</sup> even though cholinium chloride typically displays a thermodynamically ideal

behavior in these systems.<sup>6,22</sup> Its attractiveness as a DES component stems from its low toxicity,<sup>23</sup> high biodegradability,<sup>24</sup> and low melting enthalpy (4.3 kJ/mol),<sup>25</sup> causing it to present a steep solid–liquid equilibrium line and, thus, a sharp melting temperature depression effect.

The nonideality of a liquid mixture arises from the establishment of intermolecular interactions of different strength than the interactions the compounds establish with themselves in their pure liquid phases. Since negative deviations to ideality are the basis for classifying an ES as *deep*, our research group has been focused on understanding the interactions between DES components, aiming at rationalizing the design of true deep eutectic solvents.

Recently, we proposed a new type of DES (type V) based on nonionic substances.<sup>26</sup> Despite the structural similarity of its components, the system thymol/menthol presents large negative

Received: March 17, 2020

Revised: April 21, 2020

Published: April 23, 2020



deviations to ideality and is an example of this new class of DES. Due to the electron withdrawing effect of the aromatic resonance of thymol, its hydroxyl group becomes more positive, with the oxygen becoming a poorer hydrogen bond acceptor and its proton becoming a better hydrogen bond donor when compared with the hydrogen bonding capability of typical alcohols (such as menthol). Hence, thymol and menthol establish a stronger hydrogen bond network than those present in the liquid phase of the pure components. We have also identified mixtures in which tetrabutylammonium chloride ( $[N_{4,4,4,4}]Cl$ ) behaves as a chloride donating agent,<sup>27</sup> analogous to the mechanism of formation of type I DES. An example is the system  $[N_{1,1,1,1}]Cl/[N_{4,4,4,4}]Cl$  with  $[N_{1,1,1,1}]Cl$  standing for tetramethylammonium chloride, which presents large negative deviations to ideality<sup>27</sup> due to a synergetic share of the available chloride ions, in which the coordination number of chloride anions around the  $[N_{1,1,1,1}]^+$  cation increases (when compared to its pure liquid phase) and decreases around the  $[N_{4,4,4,4}]^+$  cation (in comparison to its pure liquid phase). This phenomenon, as will be shown here, can be explored to design novel type III deep eutectic solvents.

The objective of this work is to show that the current understanding of the molecular mechanisms behind DES formation, with emphasis on DES of types III and V, allows for an informed choice of *liquefying agents*, i.e., compounds that induce negative deviations to ideality in other solid compounds, originating a liquid mixture. Fatty acids (and carboxylic acids in general) are both hydrogen bond donors and acceptors, with the possibility of forming dimers in their pure liquid phases. Likewise, fatty alcohols are also both good hydrogen bond donors and acceptors. Their simple structure, minimizing the possibility of other specific interactions that could create difficulties in the interpretation of the results, and their melting points above room temperature make them attractive model compounds for this study.

In this work, a set of experimental solid–liquid equilibrium data taken from the literature, complemented with new data herein measured, is used to rationalize the liquefaction of fatty acids or alcohols using the deep eutectic solvent approach. Fatty acids (tetradecanoic acid, hexadecanoic acid, and octadecanoic acid) and fatty alcohols (tetradecan-1-ol, hexadecan-1-ol, and octadecan-1-ol) are here used as model compounds to be liquefied and menthol, thymol, cholinium chloride (ChCl),  $[N_{1,1,1,1}]Cl$ , or  $[N_{4,4,4,4}]Cl$  as compounds to induce the liquefaction. The identification of the dominant molecular interactions present on these systems will help understand the behavior of a plethora of other systems and will pave the way to the design of novel DES that are not just ideal mixtures of compounds forming, in some cases, eutectic solvents.

## 2. METHODS

**2.1. Chemicals.** The substances experimentally used in this work are reported in Table 1, along with their supplier and purity (mass %). Due to their hygroscopicity,  $[N_{1,1,1,1}]Cl$  and  $[N_{4,4,4,4}]Cl$  were dried before use by stirring in a vacuum (0.1 Pa) at room temperature (298 K) for at least 72 h. The remaining compounds were used as received. The water content of the substances was measured using a Metrohm 831 Karl Fischer coulometer, with the analyte Hydranal Coulomat AG from Riedel-de-Haen.

**2.2. Solid–Liquid Phase Diagram Measurement.** To study liquefaction by forming type V DES, the solid–liquid equilibrium (SLE) phase diagrams of the binary systems composed of thymol or (–)-menthol (menthol) and tetradecan-1-ol

**Table 1. List of Substances Experimentally Used in This Work along with Their CAS Number, Supplier, Mass Purity, and Water Content**

substance	CAS number	supplier	purity	water content (ppm)
$[N_{1,1,1,1}]Cl$	75-57-0	Sigma-Aldrich	97%	2957
$[N_{4,4,4,4}]Cl$	1112-67-0	Sigma-Aldrich	97%	5758
thymol	89-83-8	TCI	>99%	185
(–)-menthol	2216-51-5	Acros Organics	99.5%	79
tetradecanoic acid	544-63-8	Acros Organics	99%	0
hexadecanoic acid	57-10-3	Aldrich	99%	13
octadecanoic acid	57-11-4	Sigma-Aldrich	99%	12
tetradecan-1-ol	112-72-1	Alfa Aesar	98%	66
hexadecan-1-ol	36653-82-4	Alfa Aesar	98%	6
octadecan-1-ol	112-92-5	Sigma	99%	18

(tetradecanol), hexadecan-1-ol (hexadecanol), or octadecan-1-ol (octadecanol) were experimentally measured. Moreover, to study liquefaction by forming type III DES, the SLE phase diagram of the binary systems composed of  $[N_{1,1,1,1}]Cl$  and tetradecanol, hexadecanol, or octadecanol and composed of  $[N_{4,4,4,4}]Cl$  and tetradecanoic acid, hexadecanoic acid, octadecanoic acid, tetradecanol, hexadecanol, or octadecanol were also measured in this work.

For each binary system, mixtures were prepared covering the entire composition range. The mass of each component was weighted using an analytical balance (model ALS 220-4N from Kern) with a readability of 0.1 mg. After preparation, the samples were heated under stirring until fusion and recrystallized to obtain a homogeneous solid mixture. Then, the samples were crushed with a mortar and pestle and glass capillaries were filled with the resulting powder. The melting temperature of the sample in each glass capillary, taken as the temperature at which complete fusion is observed, was measured using the melting point device model M-565 from Büchi, with a temperature resolution of 0.1 K and a temperature gradient of 0.1 K/min. This procedure was repeated at least three times. For systems composed of either  $[N_{1,1,1,1}]Cl$  or  $[N_{4,4,4,4}]Cl$ , the sample and capillary preparation were performed inside a dry-argon glovebox to prevent atmospheric humidity contamination.

In the cases where the melting temperature of the mixture was below room temperature, the recrystallization technique was not possible. Thus, approximately 5 mg of these samples weighed using a microanalytical balance AD6 (PerkinElmer, USA, precision =  $2 \times 10^{-6}$  g) was tightly sealed in aluminum pans and their melting temperature measured using differential scanning calorimetry (DSC). A Hitachi DSC7000X model, working at atmospheric pressure, coupled with a cooling system, was used to perform the measurements. The cooling and heating rates were, respectively, 5 and 2 K/min, and each temperature was taken as the peak temperature upon heating. The DSC equipment was previously calibrated with several standards (heptane, octane, decane, 4-nitrotoluene, naphthalene, benzoic acid, diphenylacetic acid, indium, tin, caffeine, lead, zinc, potassium nitrate, water, and anthracene) with purities higher than 99 wt %.

The experimental methodologies described above have already been checked for the SLE phase diagram measurement of DES by comparing the measured data with other sources and methods<sup>28,29</sup> as well as applying thermodynamic consistency

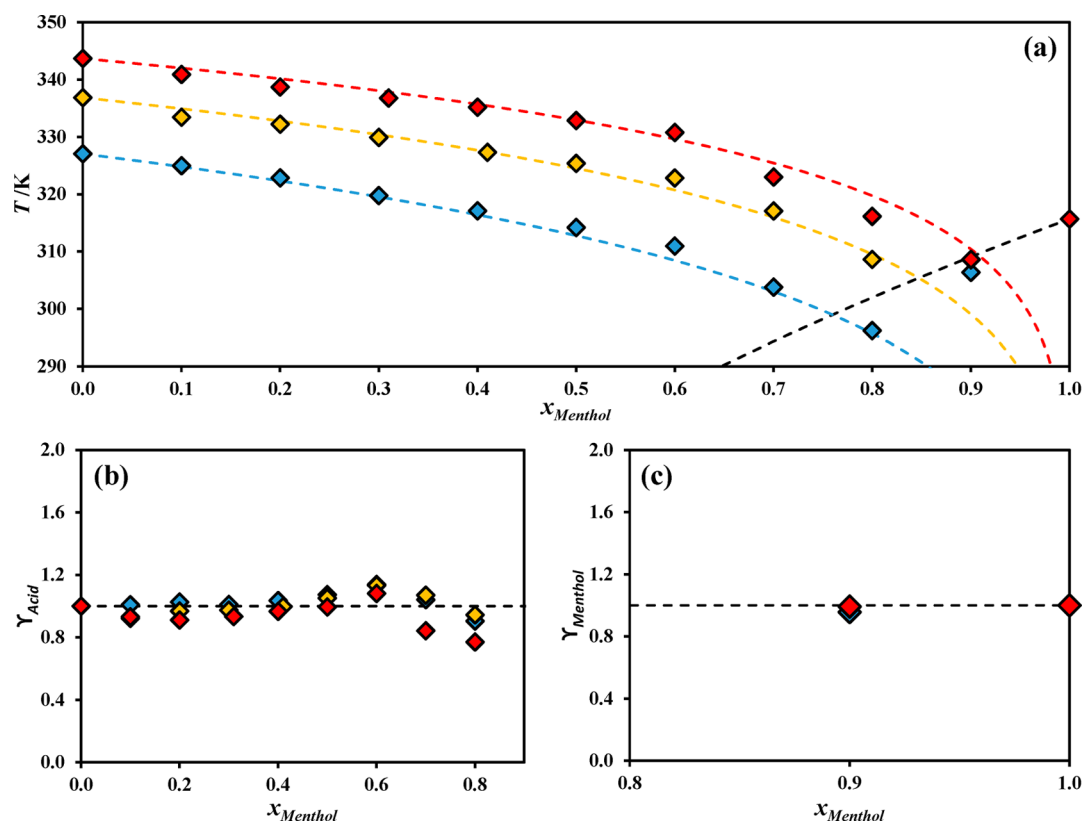


**Figure 1.** Solid–liquid phase diagrams<sup>34</sup> (a) and corresponding activity coefficients of fatty acids (b) and menthol (c) for the systems composed of menthol and tetradecanoic acid (blue  $\blacklozenge$ ), hexadecanoic acid (yellow  $\blacklozenge$ ), or octadecanoic acid (red  $\blacklozenge$ ). Dashed lines represent the ideal liquidus lines (black, menthol; blue, tetradecanoic acid; yellow, hexadecanoic acid; red, octadecanoic acid). Dotted lines represent thermodynamic ideality ( $\gamma = 1$ ).

tests.<sup>25</sup> The foundations of these methodologies are extensively described by Heffer and Tomkins.<sup>30</sup>

**2.3. Modeling.** Solid–liquid equilibrium,<sup>31–33</sup> when no solid–solid transitions are present, the components crystallize as pure substances, assuming also constant heat capacity change upon melting, and neglecting the difference between melting and triple point properties, is described by

$$\ln(x_i \gamma_i) = \frac{\Delta_m h_i}{R} \left( \frac{1}{T_{m,i}} - \frac{1}{T} \right) + \frac{\Delta_m C_{p,i}}{R} \left( \frac{T_{m,i}}{T} - \ln \frac{T_{m,i}}{T} - 1 \right) \quad (1)$$

where  $x_i$  is the mole fraction of component  $i$ ,  $\gamma_i$  is its activity coefficient in the liquid phase,  $\Delta_m h_i$  is its melting enthalpy,  $T_{m,i}$  is its melting temperature,  $\Delta_m C_{p,i}$  is its heat capacity change upon melting,  $R$  is the ideal gas constant, and  $T$  is the absolute temperature of the system. Given the small temperature difference between the melting temperature of the mixtures herein studied and those of the pure compounds, the heat capacity term is negligible,<sup>31,32</sup> with eq 1 simplifying to

$$\ln(x_i \gamma_i) = \frac{\Delta_m h_i}{R} \left( \frac{1}{T_{m,i}} - \frac{1}{T} \right) \quad (2)$$

The activity coefficients of the components in a eutectic solvent can be calculated from the experimental solid–liquid phase diagram by rearranging eq 2:

$$\gamma_i = \frac{\exp \left[ \frac{\Delta_m h_i}{R} \left( \frac{1}{T_{m,i}} - \frac{1}{T} \right) \right]}{x_i} \quad (3)$$

In this work, the activity coefficients were calculated using eq 3 and the melting properties listed in Table S1. Even for the cases where the activity coefficients were already reported in the literature, they were herein recalculated using the melting properties of Table S1 to perform consistent comparisons between all systems.

### 3. DISCUSSION

**3.1. Liquefying Acids and Alcohols by Forming Type V DES.** Due to the nonionic nature of type V DES, the interactions established between their components are simpler to understand and discuss, and our analysis starts with these systems. The solid–liquid phase diagram of menthol and the model fatty acids, taken from the literature,<sup>34</sup> are depicted in Figure 1, along with the corresponding activity coefficients estimated from eq 3, as described in section 2.3.

Figure 1 shows that both fatty acids and menthol behave ideally when mixed, with only mild deviations to ideality presented by the acids for high menthol concentration. Therefore, the molecular interactions established in the mixture are similar and of the same strength to those present in the pure component liquid phases (hydrogen bonding between hydroxyl groups of similar nature). As such, and even though the system menthol/tetradecanoic acid presents a eutectic temperature around room temperature (ca. 296 K), menthol fails at forming deep eutectic solvents with the organic acids studied.

The solid–liquid phase diagram of menthol and the model fatty alcohols were measured in this work, as described in section 2.2, and are depicted in Figure 2, along with the corresponding activity coefficients.

Similar to the menthol/fatty acid systems depicted in Figure 1, Figure 2 reveals that mixtures of menthol and fatty alcohols

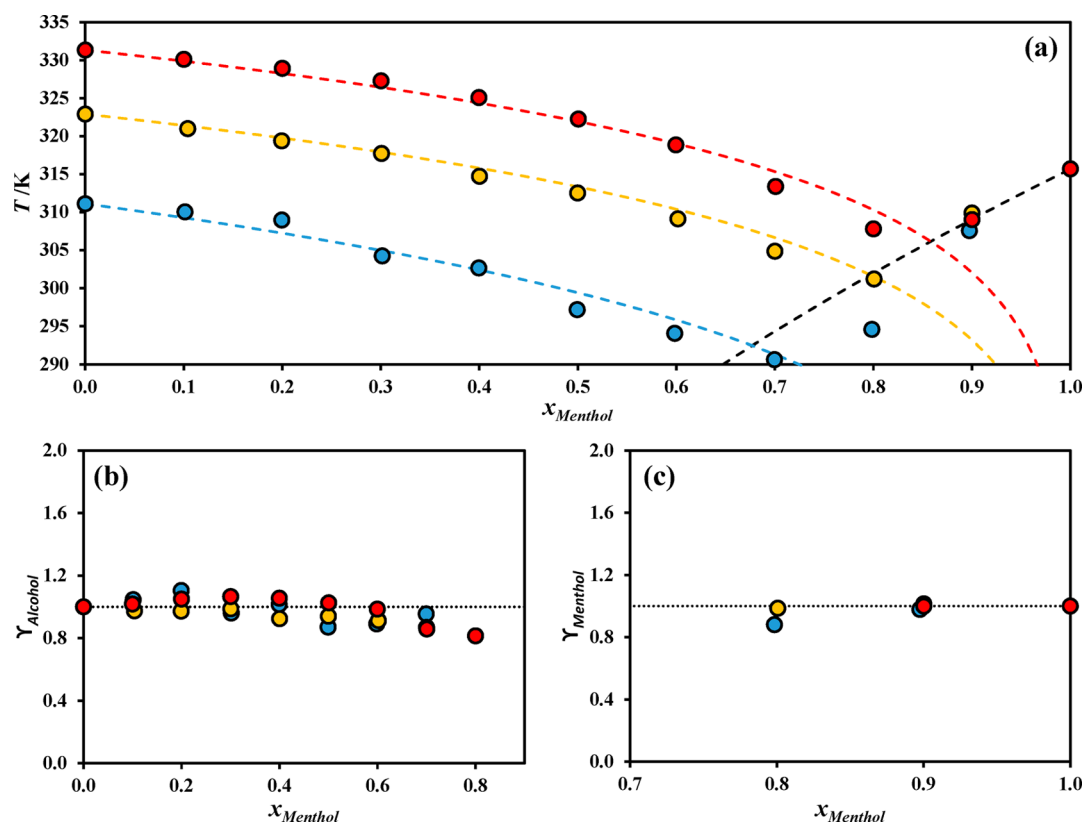


**Figure 2.** Solid–liquid phase diagrams (a) and corresponding activity coefficients of fatty alcohols (b) and menthol (c) for the systems composed of menthol and tetradecanol (blue ●), hexadecanol (yellow ●), or octadecanol (red ●). Dashed lines represent the ideal liquidus lines (black, menthol; blue, tetradecanol; yellow, hexadecanol; red, octadecanol). Dotted lines represent thermodynamic ideality ( $\gamma = 1$ ).

behave ideally. Again, the molecular interactions between menthol and the fatty alcohols present in these systems are comparable in strength to those found in the liquid phases of the pure components.

The results reported in Figures 1 and 2 reassert that the existence of hydrogen bonds between the two components of a mixture does not guarantee the presence of negative deviations to ideality and, thus, the formation of deep eutectic solvents. For this to happen, the interactions established between the components must be stronger than those present in the pure compound liquid phases. Within the framework of type V DES, these results show that aliphatic alcohols such as menthol, being hydrogen bond donors and acceptors of average strength able to establish strong interactions with themselves in their pure liquid phases, are not useful to liquefy other substances with hydroxyl and/or carboxyl groups by causing deviations to thermodynamic ideality. This conclusion is in line with our previous work, where it was shown that menthol was not responsible for the significant negative deviations to ideality present in the thymol/menthol system.<sup>26</sup> It is also in good agreement, and helps explain, previous reports of SLE phase diagrams of menthol forming ideal liquid mixtures with various other compounds.<sup>34–39</sup>

Having discussed the effect of menthol on organic acids and alcohols, the focus now shifts to thymol (see Figure S2 for both structures). Unlike menthol, thymol has a hydrogen bond capability unbalance: it is a stronger hydrogen bond donor and a weaker hydrogen bond acceptor than other hydroxyl-containing nonphenolic compounds.<sup>26</sup> The solid–liquid phase diagrams of thymol and the model fatty acids, taken from the literature,<sup>34</sup> are depicted in Figure 3, along with the corresponding activity coefficients.

Despite its hydrogen bond donning strength, Figure 3 shows that thymol cannot induce negative deviations to ideality in the model fatty acids and, thus, cannot form deep eutectic solvents with these substances. In fact, and unlike menthol/acid systems, the fatty acids studied present small positive deviations to ideality for high thymol concentration. Since the principal structural difference between thymol and menthol is that the former is a stronger hydrogen bond donor and a weaker hydrogen bond acceptor, the different activity coefficient results from Figures 1b and 3b suggest that fatty acids are acting as the hydrogen bond donors and thymol/menthol as the hydrogen bond acceptors. Menthol being a better hydrogen bond acceptor than thymol<sup>26</sup> induces the small negative deviations seen in Figure 1b.

The solid–liquid phase diagrams of thymol with the model fatty alcohols were measured in this work, as described in section 2.2, and are depicted in Figure 4, together with the corresponding activity coefficients.

The phase diagrams depicted in Figure 4 demonstrate the usefulness of thymol as a liquefying agent by forming DES of type V. Because thymol is a stronger hydrogen bond donor than the fatty alcohols, it can induce large deviations to ideality on the aliphatic alcohols by forming hydrogen bonds that are stronger than those present in the pure compounds, as also shown in a previous work for the mixture thymol–menthol,<sup>26</sup> leading to deep eutectic solvents of type V. Hydrophobic deep eutectic solvents, proposed for the first time by van Osch et al.,<sup>40</sup> expand the applicability of DES, since most previously reported in the literature are choline-based and hence hydrophilic. In this respect, the new DES reported in Figure 4 are important, since they are formed by hydrophobic substances, echoing the importance of



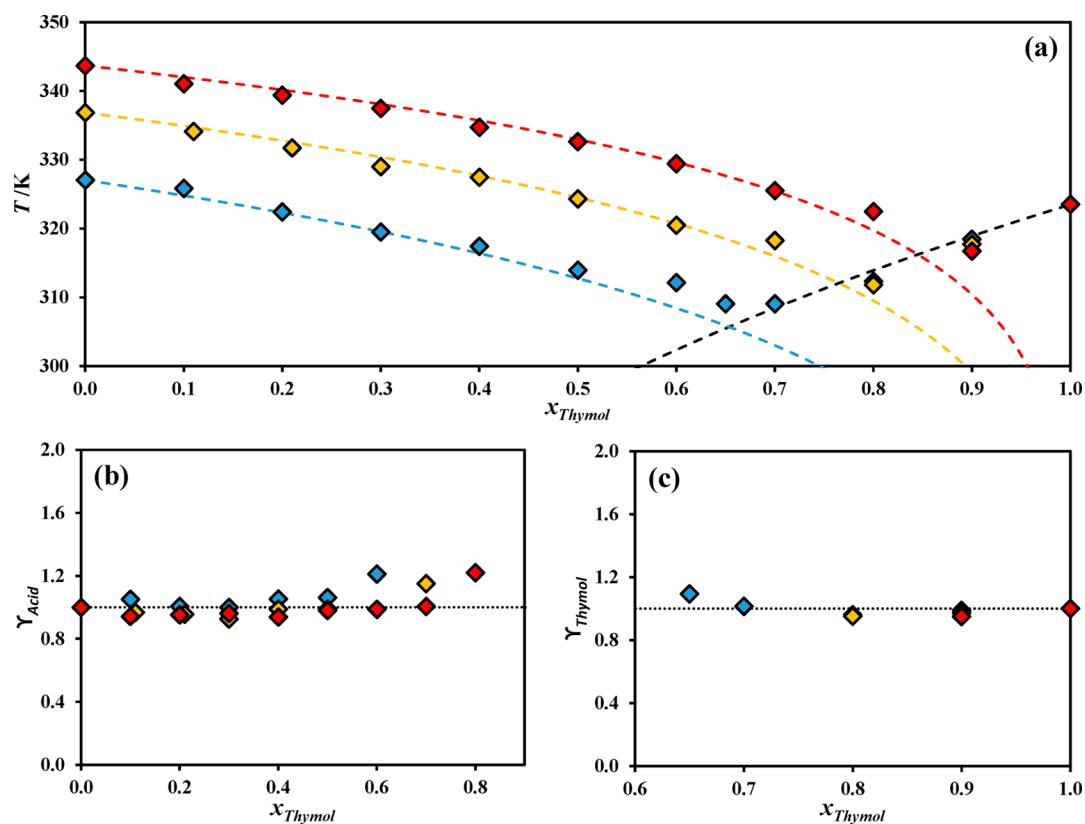


**Figure 3.** Solid–liquid phase diagrams<sup>34</sup> (a) and corresponding activity coefficients of fatty acids (b) and thymol (c) for the systems composed of thymol and tetradecanoic acid (blue  $\blacklozenge$ ), hexadecanoic acid (yellow  $\blacklozenge$ ), or octadecanoic acid (red  $\blacklozenge$ ). Dashed lines represent the ideal liquidus lines (black, thymol; blue, tetradecanoic acid; yellow, hexadecanoic acid; red, octadecanoic acid). Dotted lines represent thermodynamic ideality ( $\gamma = 1$ ).

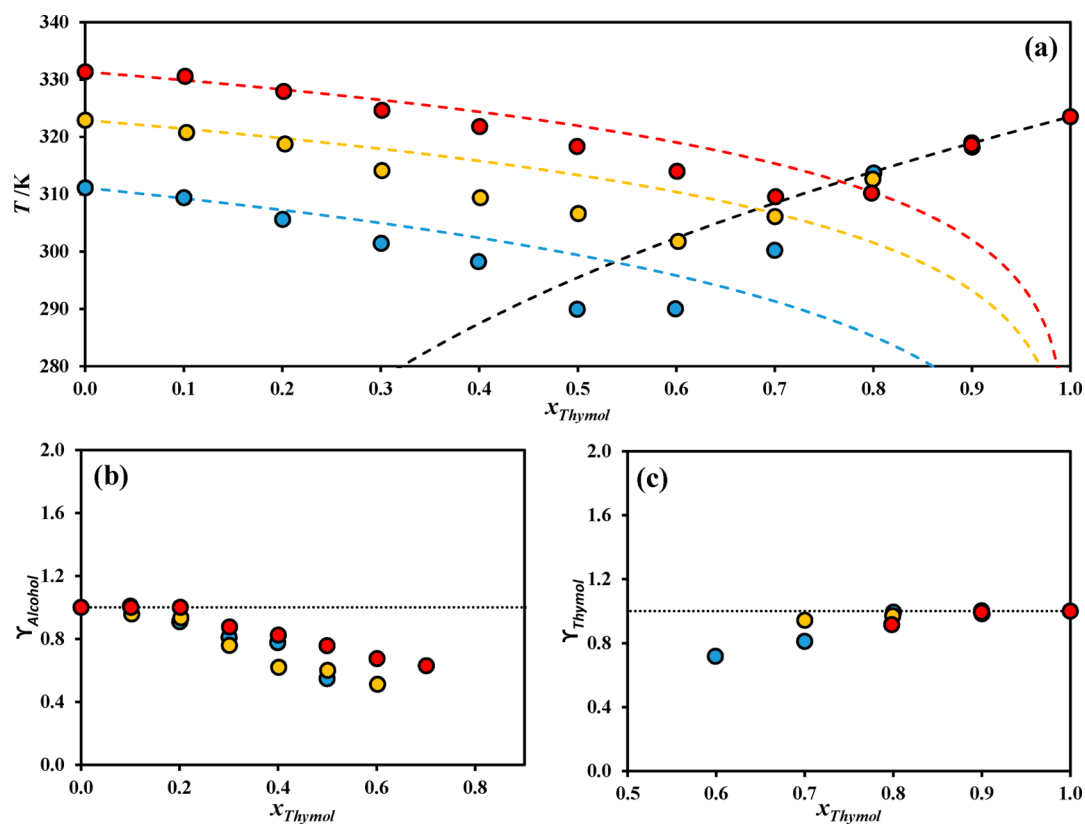


**Figure 4.** Solid–liquid phase diagrams (a) and corresponding activity coefficients of fatty alcohols (b) and thymol (c) for the systems composed of thymol and tetradecanol (blue  $\bullet$ ), hexadecanol (yellow  $\bullet$ ), or octadecanol (red  $\bullet$ ). Dashed lines represent the ideal liquidus lines (black, thymol; blue, tetradecanol; yellow, hexadecanol; red, octadecanol). Dotted lines represent thermodynamic ideality ( $\gamma = 1$ ).

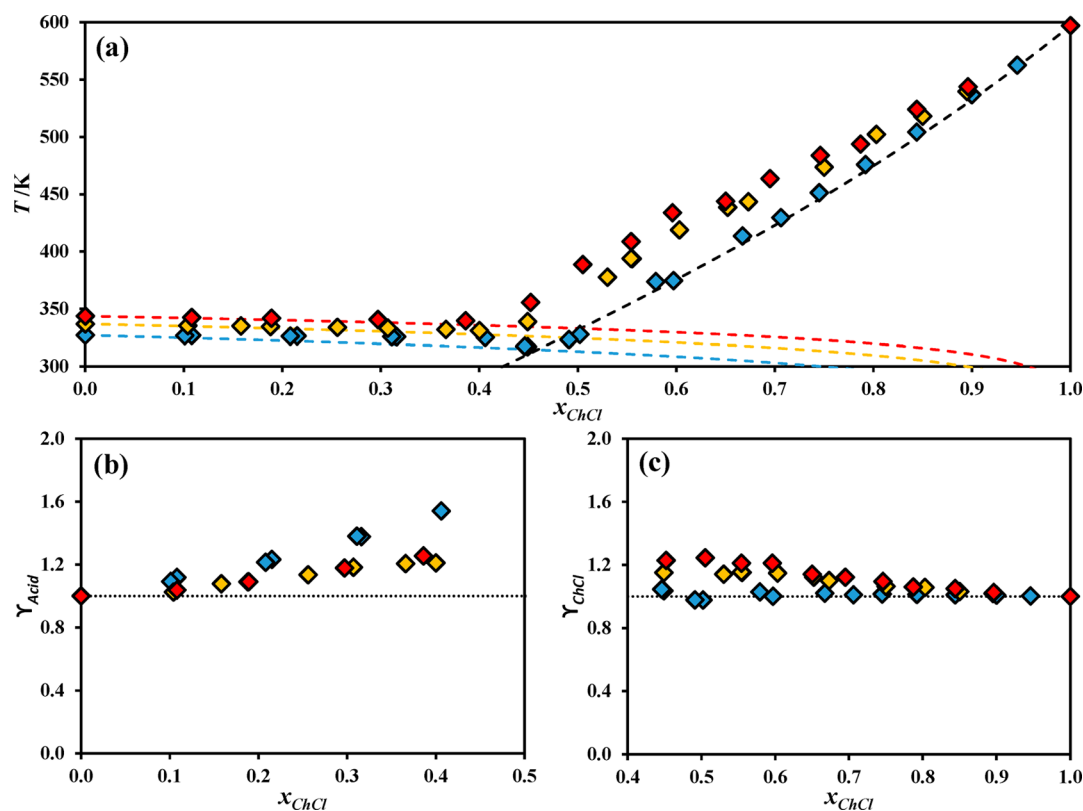


**Figure 5.** Solid–liquid phase diagrams<sup>28</sup> (a) and corresponding activity coefficients of fatty acids (b) and ChCl (c) for the systems composed of ChCl and tetradecanoic acid (blue  $\blacklozenge$ ), hexadecanoic acid (yellow  $\blacklozenge$ ), or octadecanoic acid (red  $\blacklozenge$ ). Dashed lines represent the ideal liquidus lines (black, ChCl; blue, tetradecanoic acid; yellow, hexadecanoic acid; red, octadecanoic acid). Dotted lines represent thermodynamic ideality ( $\gamma = 1$ ).

type V DES, and the informed selection of the compounds of the eutectic solvent mixture, in the preparation of novel hydrophobic solvents.

**3.2. Liquefying Alcohols and Acids by Forming Type III DES.** After showing how the type V DES framework can be used in the liquefaction of organic alcohols, yet failing, with the liquefying agents studied, at forming deep eutectic solvents with the fatty acids, type III DES are now discussed. We start by analyzing the prototypical DES-forming component: cholinium chloride. It has been previously proposed that the thermodynamic behavior of the prototypical cholinium chloride/urea DES is governed by a hydrogen bond between two protons of urea and a chloride anion,<sup>41</sup> which is a behavior reminiscent of the chloride transfer in the type I DES-analogous ionic liquid mixtures mentioned in the Introduction.<sup>27</sup>

To investigate if cholinium chloride is able to form DES with fatty acids, Figure 5 depicts their binary solid–liquid phase diagrams<sup>28</sup> and the corresponding activity coefficients.

Excluding the ChCl/tetradecanoic acid system in which cholinium chloride behaves ideally, Figure 5 reveals that both cholinium chloride and fatty acids present significant positive deviations to ideality when mixed. To investigate if, unlike the ChCl/acid systems, cholinium chloride is able to form DES with fatty alcohols, Figure 6 depicts the solid–liquid phase diagrams of these systems, taken from the literature,<sup>28</sup> along with the corresponding activity coefficients.

The results reported in Figure 6 are similar to those shown in Figure 5, with the fatty alcohols presenting large positive deviations to ideality. However, cholinium chloride now shows either an ideal behavior or small negative deviations to ideality. These results confirm that cholinium chloride does not present a

particular ability to establish new, and stronger than in pure, intermolecular interactions in mixtures.

Since these results show that cholinium chloride cannot form deep eutectic solvents with the fatty acids or alcohols studied,  $[N_{1,1,1,1}]\text{Cl}$  will be now considered. This is an interesting compound to discuss, since it is structurally similar to cholinium chloride, with the sole difference being the hydroxyethyl group of the cholinium cation replaced by a methyl group. Thus, by studying  $[N_{1,1,1,1}]\text{Cl}$ -based systems, the effect of the choline hydroxyl group can be probed while checking for DES formation by charge transfer. Figure 7 depicts the solid–liquid phase diagrams of  $[N_{1,1,1,1}]\text{Cl}$  and the model fatty acids, taken from the literature,<sup>29</sup> along with the corresponding activity coefficients.

The impact of the hydroxyl group present in cholinium chloride is quite significant, as the comparison of Figures 5 and 7 reveals. While cholinium chloride presented large positive deviations to ideality when mixed with the model acids,  $[N_{1,1,1,1}]\text{Cl}$  presents the opposite behavior, i.e., large negative deviations to ideality. Despite this change in behavior of the liquefying agent, the model fatty acids still show positive deviations to ideality identical to those found in the ChCl-based systems. This suggests that the hydroxyl group endows cholinium chloride with stronger interactions in its pure phase, namely, hydrogen bonding between the chloride anion and the highly positive hydroxyl group. By removing this effect in  $[N_{1,1,1,1}]\text{Cl}$ , the hydrogen bonding with the fatty acids becomes more favorable than its interactions in the pure liquid phase, resulting in the negative deviations seen.

To check if the absence of a hydroxyl group in  $[N_{1,1,1,1}]\text{Cl}$  also affects the fatty alcohol systems, Figure 8 depicts the solid–liquid phase equilibrium of  $[N_{1,1,1,1}]\text{Cl}$  and the fatty alcohols, along with the corresponding activity coefficients.

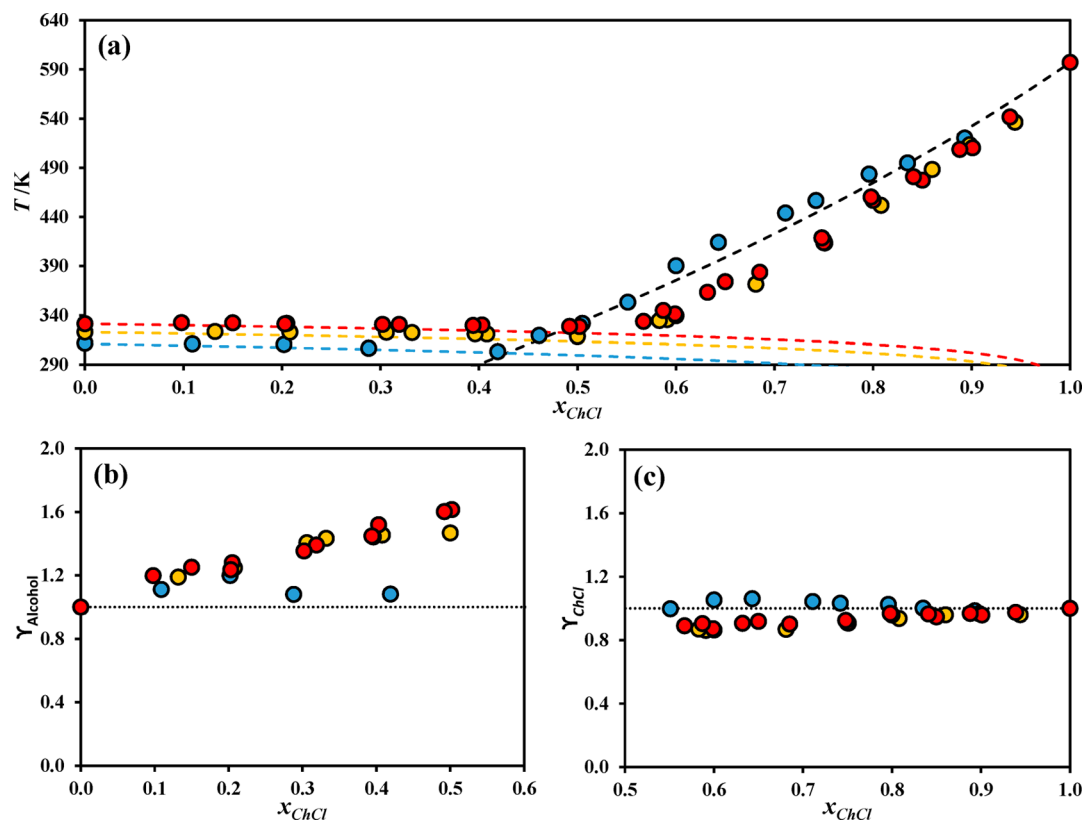


**Figure 6.** Solid–liquid phase diagrams<sup>28</sup> (a) and corresponding activity coefficients of fatty alcohols (b) and ChCl (c) for the systems composed of ChCl and tetradecanol (blue ●), hexadecanol (yellow ●), or octadecanol (red ●). Dashed lines represent the ideal liquidus lines (black, ChCl; blue, tetradecanol; yellow, hexadecanol; red, octadecanol-1-ol). Dotted lines represent thermodynamic ideality ( $\gamma = 1$ ).

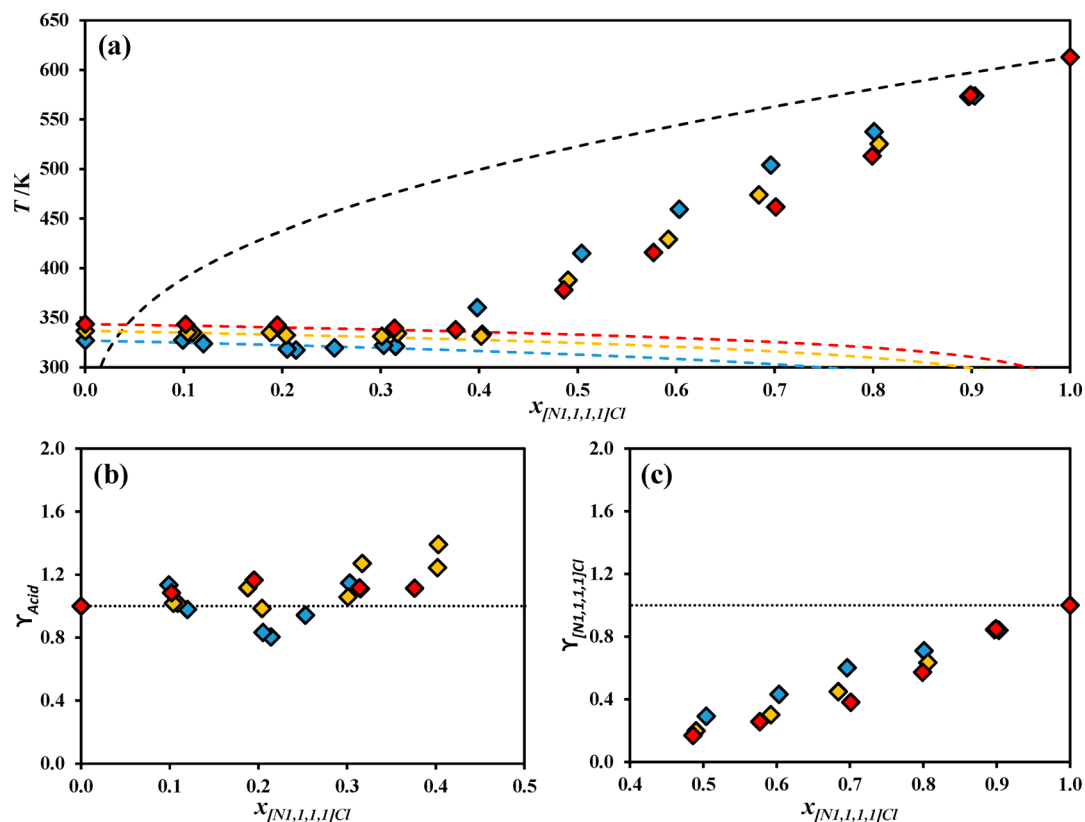


**Figure 7.** Solid–liquid phase diagrams<sup>29</sup> (a) and corresponding activity coefficients of fatty acids (b) and  $[N_{1,1,1,1}]Cl$  (c) for the systems composed of  $[N_{1,1,1,1}]Cl$  and tetradecanoic acid (blue ◆), hexadecanoic acid (yellow ◆), or octadecanoic acid (red ◆). Dashed lines represent the ideal liquidus lines (black,  $[N_{1,1,1,1}]Cl$ ; blue, tetradecanoic acid; yellow, hexadecanoic acid; red, octadecanoic acid). Dotted lines represent thermodynamic ideality ( $\gamma = 1$ ).

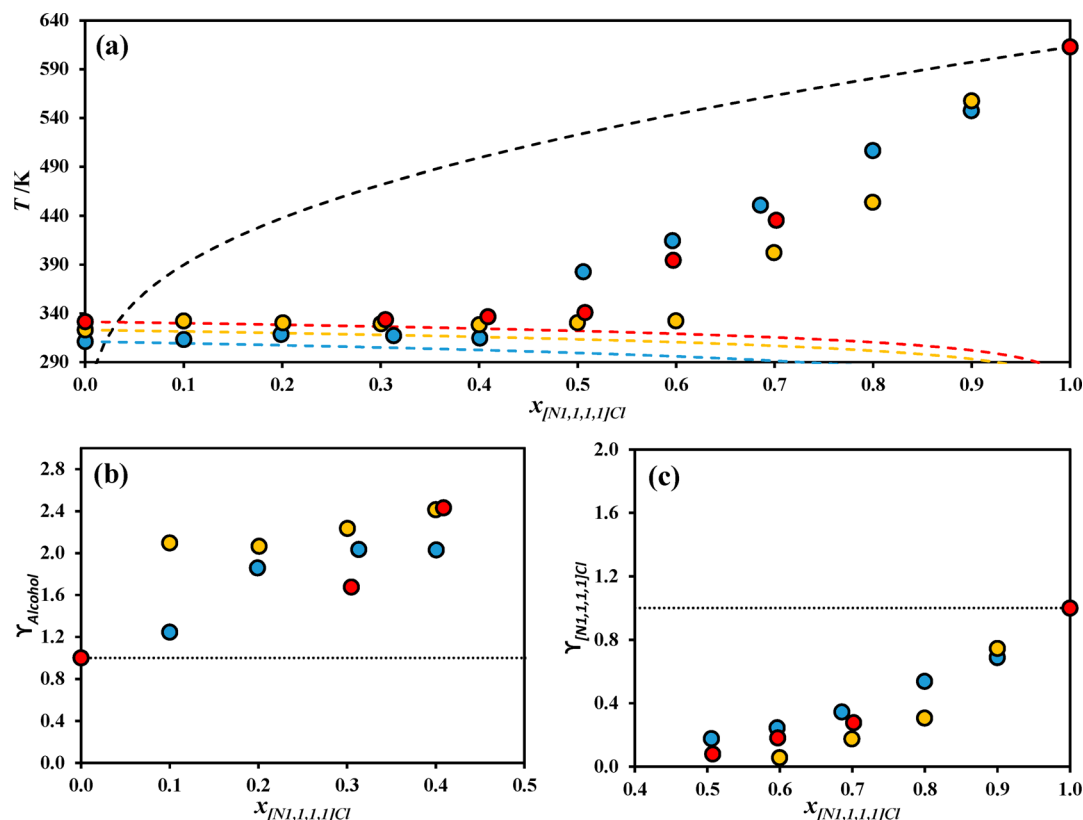


**Figure 8.** Solid–liquid phase diagrams (a) and corresponding activity coefficients of fatty alcohols (b) and  $[N_{1,1,1,1}]Cl$  (c) for the systems composed of  $[N_{1,1,1,1}]Cl$  and tetradecanol (blue ●), hexadecanol (yellow ●), or octadecanol (red ●). Dashed lines represent the ideal liquidus lines (black,  $[N_{1,1,1,1}]Cl$ ; blue, tetradecanol; yellow, hexadecanol; red, octadecanol). Dotted lines represent thermodynamic ideality ( $\gamma = 1$ ).

As observed for the systems of  $[N_{1,1,1,1}]Cl$  and fatty acids, the absence of a hydroxyl group in the tetramethylammonium cation results in very large deviations to ideality. Working under the assumption that the chloride anion is a stronger hydrogen bond acceptor than the hydroxyl groups of the fatty acids and alcohols studied (this will be later proven using  $[N_{4,4,4,4}]Cl$ ),  $COOH \cdots Cl$  or  $COH \cdots Cl$  interactions should lead to negative deviations to ideality presented by the acids/alcohols. On the contrary, the acids/alcohols in these systems show positive deviations to ideality, suggesting that  $COOH \cdots Cl$  or  $COH \cdots Cl$  interactions are not occurring.

Having seen that cholinium chloride is unable to form deep eutectic solvents with the model acids and alcohols studied due to its hydroxyl group and that  $[N_{1,1,1,1}]Cl$  produces highly asymmetrical systems with regard to activity coefficients,  $[N_{4,4,4,4}]Cl$  is now discussed.  $[N_{4,4,4,4}]Cl$  has been shown to behave as a chloride donating agent, with its cation being able to form apolar domains depleted in chloride anions.<sup>27</sup> In this work, the solid–liquid phase diagrams of the systems composed by  $[N_{4,4,4,4}]Cl$  and the model fatty acids were measured and are depicted in Figure 9.

The results reported in Figure 9 are extremely interesting. On the contrary to what was observed for all systems previously discussed, for the first time, negative deviations to ideality are present in the carboxylic acids. The  $[N_{4,4,4,4}]Cl$ , however, presents either a near-ideal behavior or even weak positive deviations to ideality. This behavior is reminiscent of that previously observed in the  $[N_{1,1,1,1}]Cl/[N_{4,4,4,4}]Cl$  system,<sup>27</sup> supporting the idea that chloride anions are being transferred from the  $[N_{4,4,4,4}]$  cation to the carboxylic acid head, engaging in stronger hydrogen bonds than those present in the pure acid liquid phases.

Bearing in mind the success of  $[N_{4,4,4,4}]Cl$  in inducing negative deviations to ideality in the model acids studied, the alcohol-based systems are now analyzed. The solid–liquid phase diagrams of these systems were measured in this work and are depicted in Figure 10, along with the corresponding activity coefficients. As can be seen, the behavior of  $[N_{4,4,4,4}]Cl$  mixed with fatty alcohols is quite similar to that observed with fatty acids. Again,  $[N_{4,4,4,4}]Cl$  is able to induce negative deviations to ideality in the alcohols, while retaining a near-ideal behavior or showing weak positive deviations to ideality.

The thermodynamic behavior of the  $[N_{4,4,4,4}]Cl$ -based systems and the  $[N_{1,1,1,1}]Cl$ -based systems is essentially opposite.  $[N_{1,1,1,1}]Cl$  formed highly asymmetrical deep eutectic solvents with the model fatty acids/alcohols studied, presenting severe negative deviations to ideality itself but failing to induce them in the other component. Contrary to this behavior,  $[N_{4,4,4,4}]Cl$  induces strong negative deviations to ideality in the organic molecules but shows itself weak positive deviations to ideality. Such a drastic difference in thermodynamic behavior suggests that the molecular interactions are fundamentally different in those two sets of systems.

Based on the results of our previous work,<sup>27</sup> given the weak interaction between the cation and anion in  $[N_{4,4,4,4}]Cl$ , it is expected that this compound donates chloride anions to the organic acids and alcohols, establishing hydrogen bonds that are stronger than those present in the acid/alcohol pure liquid phases. Since the cation of  $[N_{1,1,1,1}]Cl$  is much more densely charged, it is unable to similarly donate chloride anions, functioning as the receiving end of chloride anions in the  $[N_{1,1,1,1}]Cl/[N_{4,4,4,4}]Cl$  system, as previously shown.<sup>27</sup> Considering that  $[N_{1,1,1,1}]Cl$  shows severe negative deviations to ideality and considering that the



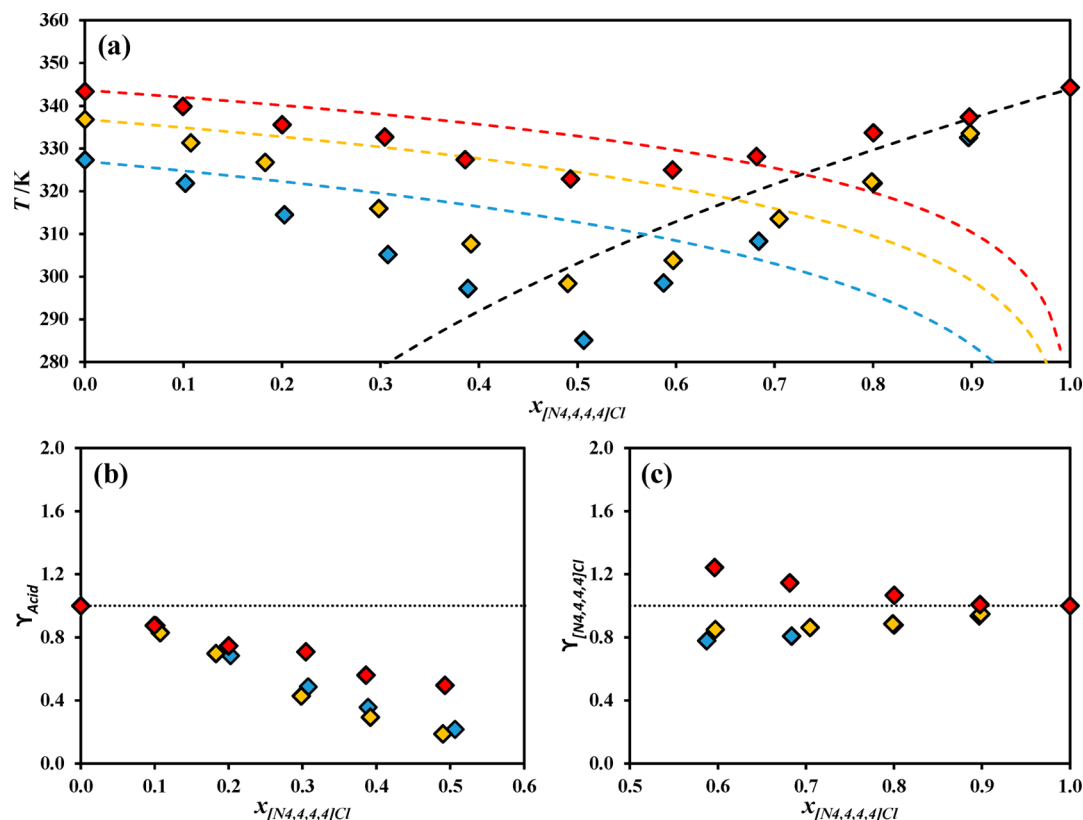


**Figure 9.** Solid–liquid phase diagrams (a) and corresponding activity coefficients of fatty acids (b) and  $[N_{4,4,4,4}]Cl$  (c) for the systems composed of  $[N_{4,4,4,4}]Cl$  and tetradecanoic acid (blue  $\blacklozenge$ ), hexadecanoic acid (yellow  $\blacklozenge$ ), or octadecanoic acid (red  $\blacklozenge$ ). Dashed lines represent the ideal liquidus lines (black,  $[N_{4,4,4,4}]Cl$ ; blue, tetradecanoic acid; yellow, hexadecanoic acid; red, octadecanoic acid). Dotted lines represent thermodynamic ideality ( $\gamma = 1$ ).

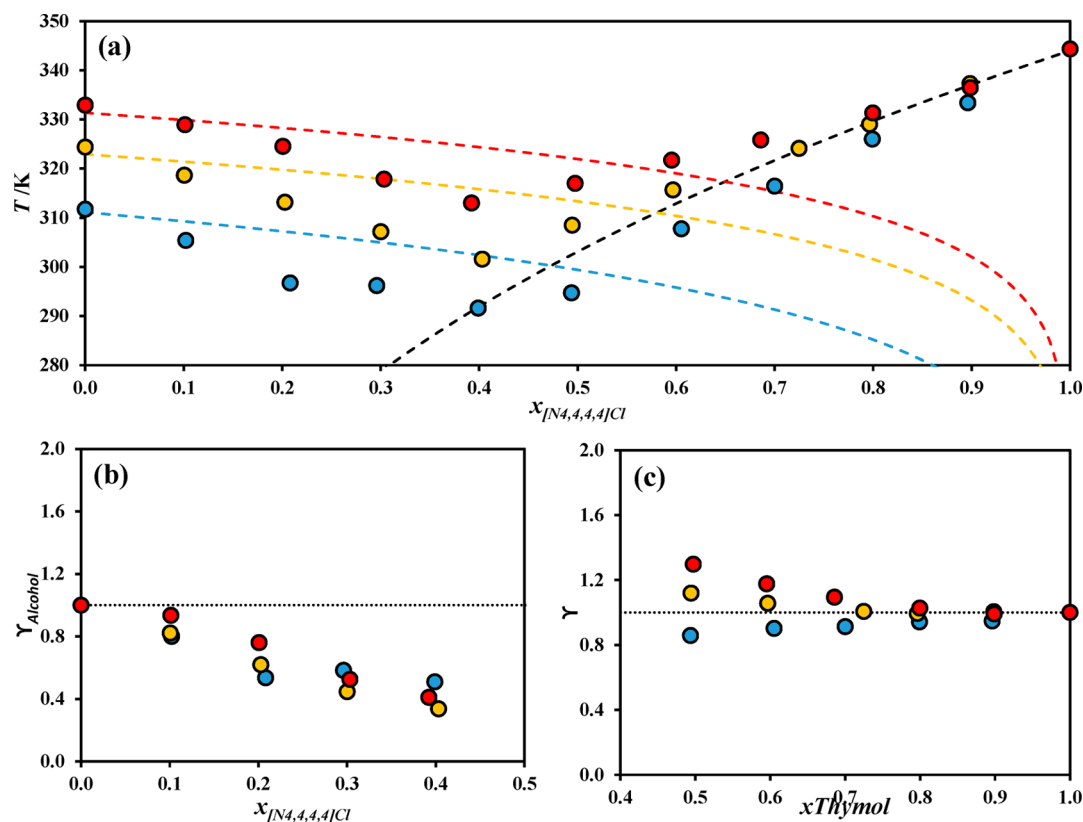


**Figure 10.** Solid–liquid phase diagrams (a) and corresponding activity coefficients of fatty alcohols (b) and  $[N_{4,4,4,4}]Cl$  (c) for the systems composed of  $[N_{4,4,4,4}]Cl$  and tetradecanol (blue  $\bullet$ ), hexadecanol (yellow  $\bullet$ ), or octadecanol (red  $\bullet$ ). Dashed lines represent the ideal liquidus lines (black,  $[N_{4,4,4,4}]Cl$ ; blue, tetradecanol; yellow, hexadecanol; red, octadecanol-1-ol). Dotted lines represent thermodynamic ideality ( $\gamma = 1$ ).

acids and alcohols presented severe positive deviations to ideality (which indicates that the new interactions established in the mixture are weaker than those present in their pure liquid phase), it is concluded that the cation of  $[N_{1,1,1,1}]Cl$  is interacting with the negative zones of the organic molecules (lone pairs of the oxygen atoms), further stabilizing itself by withdrawing additional negative charge but preventing the hydrogen bonding between the organic molecules, leading to the asymmetrical deviations to ideality seen in these systems.

#### 4. CONCLUSIONS

Throughout this work, the feasibility of forming deep eutectic solvents based on fatty alcohols or acids was studied using different liquefying agents. This work reiterates the importance of studying the solid–liquid phase diagrams of deep eutectic solvents in order to understand their molecular interactions and the origin of their deviations to ideality and rationalizing the search for new DES.

Regarding type V DES, it was shown that thymol induces negative deviations to ideality in organic alcohols, allowing the design of new hydrophobic deep eutectic solvents. Furthermore, it was shown that menthol forms ideal mixtures with the fatty acids or alcohols studied, as expected due to the similarity of the interactions established in these mixtures to those established in the pure component liquid phases, confirming that the existence of hydrogen bonding networks in eutectic solvents does not guarantee negative deviations to ideality and, thus, does not mean that the eutectic solvent is deep.

In terms of type III DES, it was shown that cholinium chloride is unable to form deep eutectic solvents with either fatty acids or alcohols. Using  $[N_{1,1,1,1}]Cl$ , it was shown that the ideal behavior of cholinium chloride in the systems studied stems from its hydroxyethyl group, which allows for strong cation–anion interactions in its pure, hypothetical, liquid phase. Thus, although due to its low melting enthalpy and green properties cholinium chloride can be seen as a generic eutectic solvent-forming compound, it is however unable to form deep eutectic solvents with organic acids or alcohols. Finally, it was shown that  $[N_{4,4,4,4}]Cl$  forms deep eutectic solvents with the fatty acids and alcohols studied.

Within the liquefying-agent concept, this work demonstrates the usefulness of thymol (type V DES) and  $[N_{4,4,4,4}]Cl$  (type III DES) in forming deep eutectic solvents with organic acids and alcohols, leading to the liquefaction of these substances. More specifically, liquid mixtures below room temperature (298 K) were obtained for tetradecanol when mixed with either thymol or  $[N_{4,4,4,4}]Cl$  and for tetradecanoic and hexadecanoic acids when mixed with  $[N_{4,4,4,4}]Cl$ .

An understanding of the interactions between liquefying agents and organic substances allows for the design of novel DES of importance to green chemistry. This work highlights some of these interactions and liquefying agents that can induce them, but further investigation is still required to compile a full body of these favorable interactions for classes of compounds other than acids or alcohols.

#### ■ ASSOCIATED CONTENT

##### SI Supporting Information

The Supporting Information is available free of charge at <https://pubs.acs.org/doi/10.1021/acs.jpbc.0c02386>.

Table S1, melting properties; Table S2, detailed experimental results; Figures S1 and S2, chemical structures (PDF)

#### ■ AUTHOR INFORMATION

##### Corresponding Author

João A. P. Coutinho – CICECO – Aveiro Institute of Materials, Department of Chemistry, University of Aveiro, 3810-193 Aveiro, Portugal; [orcid.org/0000-0002-3841-743X](https://orcid.org/0000-0002-3841-743X); Email: [jcoutinho@ua.pt](mailto:jcoutinho@ua.pt)

##### Authors

Dinis O. Abranches – CICECO – Aveiro Institute of Materials, Department of Chemistry, University of Aveiro, 3810-193 Aveiro, Portugal; [orcid.org/0000-0003-0097-2072](https://orcid.org/0000-0003-0097-2072)

Renato O. Martins – CICECO – Aveiro Institute of Materials, Department of Chemistry, University of Aveiro, 3810-193 Aveiro, Portugal; [orcid.org/0000-0002-6934-3314](https://orcid.org/0000-0002-6934-3314)

Liliana P. Silva – CICECO – Aveiro Institute of Materials, Department of Chemistry, University of Aveiro, 3810-193 Aveiro, Portugal; [orcid.org/0000-0002-6636-1920](https://orcid.org/0000-0002-6636-1920)

Mónia A. R. Martins – CICECO – Aveiro Institute of Materials, Department of Chemistry, University of Aveiro, 3810-193 Aveiro, Portugal; [orcid.org/0000-0003-0748-1612](https://orcid.org/0000-0003-0748-1612)

Simão P. Pinho – Centro de Investigação de Montanha (CIMO), Instituto Politécnico de Bragança, 5300-253 Bragança, Portugal; [orcid.org/0000-0002-9211-857X](https://orcid.org/0000-0002-9211-857X)

Complete contact information is available at:

<https://pubs.acs.org/10.1021/acs.jpbc.0c02386>

##### Notes

The authors declare no competing financial interest.

#### ■ ACKNOWLEDGMENTS

This work was developed within the scope of the projects CICECO-Aveiro Institute of Materials, UIDB/50011/2020 and UIDP/50011/2020, financed by national funds through the Portuguese Foundation for Science and Technology/MCTES, and CIMO-Mountain Research Center, UIDB/00690/2020, financed by national funds through the FCT/MEC and when appropriate cofinanced by FEDER under the PT2020 Partnership Agreement. L.P.S. acknowledges FCT for her PhD grant (SFRH/BD/135976/2018).

#### ■ REFERENCES

- (1) Smith, E. L.; Abbott, A. P.; Ryder, K. S. Deep Eutectic Solvents (DESs) and Their Applications. *Chem. Rev.* **2014**, *114* (21), 11060–11082.
- (2) Abbott, A. P.; Boothby, D.; Capper, G.; Davies, D. L.; Rasheed, R. K. Deep Eutectic Solvents Formed between Choline Chloride and Carboxylic Acids: Versatile Alternatives to Ionic Liquids. *J. Am. Chem. Soc.* **2004**, *126* (29), 9142–9147.
- (3) Abbott, A. P.; Capper, G.; Davies, D. L.; Rasheed, R. K.; Tambyrajah, V. Novel Solvent Properties of Choline Chloride/urea Mixtures. *Chem. Commun.* **2003**, *9* (1), 70–71.
- (4) Abbott, A. P.; Capper, G.; Davies, D. L.; McKenzie, K. J.; Obi, S. U. Solubility of Metal Oxides in Deep Eutectic Solvents Based on Choline Chloride. *J. Chem. Eng. Data* **2006**, *51* (4), 1280–1282.
- (5) Abbott, A. P.; Harris, R. C.; Ryder, K. S.; D'Agostino, C.; Gladden, L. F.; Mantle, M. D. Glycerol Eutectics as Sustainable Solvent Systems. *Green Chem.* **2011**, *13* (1), 82–90.
- (6) Martins, M. A. R.; Pinho, S. P.; Coutinho, J. A. P. Insights into the Nature of Eutectic and Deep Eutectic Mixtures. *J. Solution Chem.* **2019**, *48* (7), 962–982.
- (7) Li, X.; Row, K. H. Development of Deep Eutectic Solvents Applied in Extraction and Separation. *J. Sep. Sci.* **2016**, *39* (18), 3505–3520.

- (8) Zainal-Abidin, M. H.; Hayyan, M.; Hayyan, A.; Jayakumar, N. S. New Horizons in the Extraction of Bioactive Compounds Using Deep Eutectic Solvents: A Review. *Anal. Chim. Acta* **2017**, *979*, 1–23.
- (9) Zhang, Y.; Ji, X.; Lu, X. Choline-Based Deep Eutectic Solvents for CO<sub>2</sub> Separation: Review and Thermodynamic Analysis. *Renewable Sustainable Energy Rev.* **2018**, *97*, 436–455.
- (10) Chandran, D.; Khalid, M.; Walvekar, R.; Mubarak, N. M.; Dharaskar, S.; Wong, W. Y.; Gupta, T. C. S. M. Deep Eutectic Solvents for Extraction-Desulphurization: A Review. *J. Mol. Liq.* **2019**, *275*, 312–322.
- (11) Hadj-Kali, M. K.; Salleh, Z.; Ali, E.; Khan, R.; Hashim, M. A. Separation of Aromatic and Aliphatic Hydrocarbons Using Deep Eutectic Solvents: A Critical Review. *Fluid Phase Equilib.* **2017**, *448*, 152–167.
- (12) Tang, B.; Zhang, H.; Row, K. H. Application of Deep Eutectic Solvents in the Extraction and Separation of Target Compounds from Various Samples. *J. Sep. Sci.* **2015**, *38* (6), 1053–1064.
- (13) del Monte, F.; Carriazo, D.; Serrano, M. C.; Gutiérrez, M. C.; Ferrer, M. L. Deep Eutectic Solvents in Polymerizations: A Greener Alternative to Conventional Syntheses. *ChemSusChem* **2014**, *7* (4), 999–1009.
- (14) Durand, E.; Lecomte, J.; Villeneuve, P. Deep Eutectic Solvents: Synthesis, Application, and Focus on Lipase-Catalyzed Reactions. *Eur. J. Lipid Sci. Technol.* **2013**, *115* (4), 379–385.
- (15) Huang, Z.-L.; Wu, B.-P.; Wen, Q.; Yang, T.-X.; Yang, Z. Deep Eutectic Solvents Can Be Viable Enzyme Activators and Stabilizers. *J. Chem. Technol. Biotechnol.* **2014**, *89* (12), 1975–1981.
- (16) Zdanowicz, M.; Wilpiszewska, K.; Sychaj, T. Deep Eutectic Solvents for Polysaccharides Processing. A Review. *Carbohydr. Polym.* **2018**, *200*, 361–380.
- (17) Shishov, A.; Bulatov, A.; Locatelli, M.; Carradori, S.; Andruch, V. Application of Deep Eutectic Solvents in Analytical Chemistry. A Review. *Microchem. J.* **2017**, *135*, 33–38.
- (18) Zhao, H.; Baker, G. A. Ionic Liquids and Deep Eutectic Solvents for Biodiesel Synthesis: A Review. *J. Chem. Technol. Biotechnol.* **2013**, *88* (1), 3–12.
- (19) Troter, D. Z.; Todorovic, Z. B.; Đokic-Stojanovic, D. R.; Stamenkovic, O. S.; Veljkovic, V. B. Application of Ionic Liquids and Deep Eutectic Solvents in Biodiesel Production: A Review. *Renewable Sustainable Energy Rev.* **2016**, *61*, 473–500.
- (20) Nkuku, C. A.; LeSuer, R. J. Electrochemistry in Deep Eutectic Solvents. *J. Phys. Chem. B* **2007**, *111* (46), 13271–13277.
- (21) Paiva, A.; Craveiro, R.; Aroso, I.; Martins, M.; Reis, R. L.; Duarte, A. R. C. Natural Deep Eutectic Solvents – Solvents for the 21st Century. *ACS Sustainable Chem. Eng.* **2014**, *2* (5), 1063–1071.
- (22) Abranches, D. O.; Larriba, M.; Silva, L. P.; Melle-Franco, M.; Palomar, J. F.; Pinho, S. P.; Coutinho, J. A. P. Using COSMO-RS to Design Choline Chloride Pharmaceutical Eutectic Solvents. *Fluid Phase Equilib.* **2019**, *497*, 71–78.
- (23) Zhao, B.-Y.; Xu, P.; Yang, F.-X.; Wu, H.; Zong, M.-H.; Lou, W.-Y. Biocompatible Deep Eutectic Solvents Based on Choline Chloride: Characterization and Application to the Extraction of Rutin from *Sophora Japonica*. *ACS Sustainable Chem. Eng.* **2015**, *3* (11), 2746–2755.
- (24) Radošević, K.; Cvjetko Bubalo, M.; Gaurina Srček, V.; Grgas, D.; Landeka Dragičević, T.; Radojčić Redovniković, I. Evaluation of Toxicity and Biodegradability of Choline Chloride Based Deep Eutectic Solvents. *Ecotoxicol. Environ. Saf.* **2015**, *112*, 46–53.
- (25) Fernandez, L.; Silva, L. P.; Martins, M. A. R.; Ferreira, O.; Ortega, J.; Pinho, S. P.; Coutinho, J. A. P. Indirect Assessment of the Fusion Properties of Choline Chloride from Solid-Liquid Equilibria Data. *Fluid Phase Equilib.* **2017**, *448*, 9–14.
- (26) Abranches, D. O.; Martins, M. A. R.; Silva, L. P.; Schaeffer, N.; Pinho, S. P.; Coutinho, J. A. P. Phenolic Hydrogen Bond Donors in the Formation of Non-Ionic Deep Eutectic Solvents: The Quest for Type V DES. *Chem. Commun.* **2019**, *55* (69), 10253–10256.
- (27) Abranches, D. O.; Schaeffer, N.; Silva, L. P.; Martins, M. A. R.; Pinho, S. P.; Coutinho, J. A. P. The Role of Charge Transfer in the Formation of Type I Deep Eutectic Solvent-Analogous Ionic Liquid Mixtures. *Molecules* **2019**, *24* (20), 3687.
- (28) Crespo, E. A.; Silva, L. P.; Martins, M. A. R.; Fernandez, L.; Ortega, J.; Ferreira, O.; Sadowski, G.; Held, C.; Pinho, S. P.; Coutinho, J. A. P. Characterization and Modeling of the Liquid Phase of Deep Eutectic Solvents Based on Fatty Acids/Alcohols and Choline Chloride. *Ind. Eng. Chem. Res.* **2017**, *56* (42), 12192–12202.
- (29) Pontes, P. V. A.; Crespo, E. A.; Martins, M. A. R.; Silva, L. P.; Neves, C. M. S. S.; Maximo, G. J.; Hubinger, M. D.; Batista, E. A. C.; Pinho, S. P.; Coutinho, J. A. P.; et al. Measurement and PC-SAFT Modeling of Solid-Liquid Equilibrium of Deep Eutectic Solvents of Quaternary Ammonium Chlorides and Carboxylic Acids. *Fluid Phase Equilib.* **2017**, *448*, 69–80.
- (30) Hefter, G. T.; Tomkins, R. P. T. *The Experimental Determination of Solubilities*; John Wiley & Sons, Ltd: Chichester, U.K., 2003.
- (31) Coutinho, J. A. P.; Andersen, S. I.; Stenby, E. H. Evaluation of Activity Coefficient Models in Prediction of Alkane Solid-Liquid Equilibria. *Fluid Phase Equilib.* **1995**, *103* (1), 23–39.
- (32) Elliott, J. R.; Lira, C. T. *Introductory Chemical Engineering Thermodynamics*, 1st ed.; Prentice Hall: Upper Saddle River, NJ, 1999.
- (33) Prausnitz, J. M.; Lichtenthaler, R. N.; Azevedo, E. G. de. *Molecular Thermodynamics of Fluid-Phase Equilibria*, 3rd ed.; Prentice Hall: Upper Saddle River, NJ, 1999.
- (34) Martins, M. A. R.; Crespo, E. A.; Pontes, P. V. A.; Silva, L. P.; Bülow, M.; Maximo, G. J.; Batista, E. A. C.; Held, C.; Pinho, S. P.; Coutinho, J. A. P. Tunable Hydrophobic Eutectic Solvents Based on Terpenes and Monocarboxylic Acids. *ACS Sustainable Chem. Eng.* **2018**, *6* (7), 8836–8846.
- (35) Martins, M. A. R.; Silva, L. P.; Schaeffer, N.; Abranches, D. O.; Maximo, G. J.; Pinho, S. P.; Coutinho, J. A. P. Greener Terpene-Terpene Eutectic Mixtures as Hydrophobic Solvents. *ACS Sustainable Chem. Eng.* **2019**, *7* (20), 17414–17423.
- (36) Alhadid, A.; Mokrushina, L.; Minceva, M. Design of Deep Eutectic Systems: A Simple Approach for Preselecting Eutectic Mixture Constituents. *Molecules* **2020**, *25* (5), 1077.
- (37) Okuniewski, M.; Padaszyński, K.; Domańska, U. (Solid + Liquid) Equilibrium Phase Diagrams in Binary Mixtures Containing Terpenes: New Experimental Data and Analysis of Several Modelling Strategies with Modified UNIFAC (Dortmund) and PC-SAFT Equation of State. *Fluid Phase Equilib.* **2016**, *422*, 66–77.
- (38) Di Prinzio, R. C.; Pontes, P. V. de A.; Costa, M. C. da; Meirelles, A. J. de A.; Batista, E. A. C.; Maximo, G. J. Phase Equilibrium of Fats and Monoterpenes and How It Affects Chocolate Quality. *J. Chem. Eng. Data* **2019**, *64* (8), 3231–3243.
- (39) Kaplun-Frischoff, Y.; Touitou, E. Testosterone Skin Permeation Enhancement by Menthol through Formation of Eutectic with Drug and Interaction with Skin Lipids. *J. Pharm. Sci.* **1997**, *86* (12), 1394–1399.
- (40) van Osch, D. J. G. P.; Zubeir, L. F.; van den Bruinhorst, A.; Rocha, M. A. A.; Kroon, M. C. Hydrophobic Deep Eutectic Solvents as Water-Immiscible Extractants. *Green Chem.* **2015**, *17* (9), 4518–4521.
- (41) Silva, L. P.; Araújo, C. F.; Abranches, D. O.; Melle-Franco, M.; Martins, M. A. R.; Nolasco, M. M.; Ribeiro-Claro, P. J. A.; Pinho, S. P.; Coutinho, J. A. P. What a Difference a Methyl Group Makes – Probing Choline-urea Molecular Interactions through Urea Structure Modification. *Phys. Chem. Chem. Phys.* **2019**, *21* (33), 18278–18289.